Available online at www.sciencedirect.com
SCIENCE DIRECT®
Coordination Chemistry Reviews 248 (2004) 135–146
COORDINATION CHEMISTRY REVIEWS
www.elsevier.com/locate/ccr

Review

Molecular insights for how preferred oxoanions bind to and stabilize transition-metal nanoclusters: a tridentate, C_3 symmetry, lattice size-matching binding model

Richard G. Finke [a,*], Saim Özkar [b]

[a] *Department of Chemistry, Colorado State University, Fort Collins, CO 80523, USA*
[b] *Department of Chemistry, Middle East Technical University, 06531 Ankara, Turkey*

Received 27 May 2003; accepted 11 August 2003

Contents

Abstract

The recent discovery of an anion efficacy series for the formation and stabilization of transition-metal $Ir(0)_n$ nanoclusters, specifically $P_2W_{15}Nb_3O_{62}^{9-} \sim SiW_9Nb_3O_{40}^{7-} > C_6H_5O_7^{3-} > [-CH_2-CH(CO_2^-)-]_n^{n-} \sim OAc^- \sim P_3O_9^{3-} \sim Cl^- \sim OH^-$—that is, polyoxoanions > citrate^{3-} > other commonly employed nanocluster stabilizing anions, raises the question of what are the underlying factors behind this preferred order of stabilizers? A brief discussion of three relevant nanocluster papers in the literature, plus a concise summary of the relevant interfacial electrochemistry and surface science literature of C_3 symmetry SO_4^{2-} binding to Ir(1 1 1) (as well as to Rh(1 1 1), Pt(1 1 1), Au(1 1 1) and Cu(1 1 1)), are presented first as key background for the lattice size-matching model which follows in which tridentate anions coordinate to transition-metal nanocluster surfaces. A table of nanocluster formation and stabilization data for tridentate oxoanion stabilizers is presented, results which allow two fundamental, previously unavailable, important insights (out of 10 total insights): (i) the premier anionic stabilizers of transition-metal(0) nanoclusters present a tridentate, facial array of oxygen atoms for coordination to the metal(0) surface; and (ii) the preferred tridentate oxoanion stabilizers of nanoclusters are those that have the best match between the ligand O–O and surface Ir–Ir distances, all other factors being equal—that is, there is a previously unappreciated, geometric, anion-to-surface-metal *lattice-size-matching component* to the best anionic stabilizers of transition-metal nanoclusters. These are the first molecular-level insights for how the to-date premier tridentate, anionic stabilizers of transition-metal nanoclusters achieve their higher level of stabilization—a non-trivial advance since there was a lack previously of molecular-level insights into how transition-metal nanoclusters are stabilized. Four experimentally testable predictions of the C_3 symmetry, lattice size-matching model for nanocluster M(1 1 1) surfaces are presented and briefly discussed. One key prediction is that HPO_4^{2-} is a heretofore unappreciated simple, effective and readily available stabilizer of Ir(0) and other transition-metal nanoclusters where there is a lattice-size match between the O–O and the surface M–M distances. Recent experimental evidence is summarized revealing that *this prediction is, in fact, true*—that is, the third key, new finding of this work is (iii) the first rational design of a new nanocluster stabilizer,

* Corresponding author. Tel.: +1-970-491-2541; fax: +1-970-491-1801.
E-mail address: rfinke@lamar.colostate.edu (R.G. Finke).

doi:10.1016/j.cct.2003.08.003

HPO_4^{2-}, one shown to be as good a stabilizer as the common nanocluster stabilizer citrate^{3-}. The C_3 symmetry, lattice size-matching model is significant in seven additional ways which are detailed in the text and summary which follows.

Keywords: Transition-metal nanocluster stabilization; Preferred stabilizer fundamental studies; Tridentate, C_3 symmetry, lattice size-matching, stabilizer-binding model; Tridentate oxoanion coordination to metal surfaces for the purposes of corrosion resistance, electrical resistance, or bonding organic coatings; Phosphating of metal surfaces

1. Introduction

Three recent publications [1–3] address, for the first time, the fundamental role of anionic-ligand stabilization of modern transition-metal nanoclusters [4,5]. Those studies evaluate the efficacy of nanocluster surface-binding anionic stabilizers according to five criteria, specifically the ability of different anionic stabilizers [1,2]: (i) to provide for a high level of kinetic control in the nanocluster synthesis (as measured by the autocatalytic growth to continuous nucleation rate constants ratio [6], k_2/k_1); (ii) to yield near-monodisperse nanoclusters (i.e., by definition nanoclusters with less than or equal to ±15% size-distributions [4]) as judged by transmission electron microscopy (TEM); (iii) to allow isolable, then fully re-dissolvable, nanoclusters without the formation of visible bulk metal; (iv) to allow the highest catalytic activity of the re-dissolved nanoclusters in the test reaction of catalytic hydrogenation; and also (v) to allow the longest catalytic lifetime, as judged by the number of total turnovers (TTOs) of cyclohexene hydrogenation. The anions which have been investigated [1,2] according to the above five criteria for transition-metal nanocluster *formation and stabilization* include the polyanions $P_2W_{15}Nb_3O_{62}^{9-}$, $SiW_9Nb_3O_{40}^{7-}$, $C_6H_5O_7^{3-}$ (citrate^{3-}), $[-CH_2-CH(CO_2^-)-]_n^{n-}$ (polyacrylate^{n-}) and $P_3O_9^{3-}$ (trimetaphosphate) plus the common monoanions, OAc^-, Cl^- and OH^-. The $P_2W_{15}Nb_3O_{62}^{9-}$, $SiW_9Nb_3O_{40}^{7-}$ and $P_3O_9^{3-}$ were all previously unknown *individual* nanocluster-stabilizing poly(oxo)anions, as well as an unprecedented *series* of nanocluster-stabilizing poly(oxo)anions, prior to recent work [1,2].

The anion efficacy series,[1,2] for the stabilization of transition-metal Ir(0) nanoclusters by the anions of primary interest to the present review, in acetone and with Bu_4N^+ counter cations, is [1,2]:

$$P_2W_{15}Nb_3O_{62}^{9-} \sim SiW_9Nb_3O_{40}^{7-} > C_6H_5O_7^{3-} > P_3O_9^{3-} \sim OH^-.$$

The above anion series raises the obvious question of what are the underlying factors behind this order of anion efficacy for the formation and stabilization of at least Ir(0) nanoclusters? It is this question that is the general focus of the present review.

It is well known from the colloidal stabilization literature that the general modes of stabilization of nanoparticles involve two broad effects as illustrated in Fig. 1: (a) Coulombic (electrostatic) repulsive stabilization towards agglomeration which opposes the van der Waals attraction of the particles, both as treated by DLVO theory[3] [7a–7c], and (b) steric

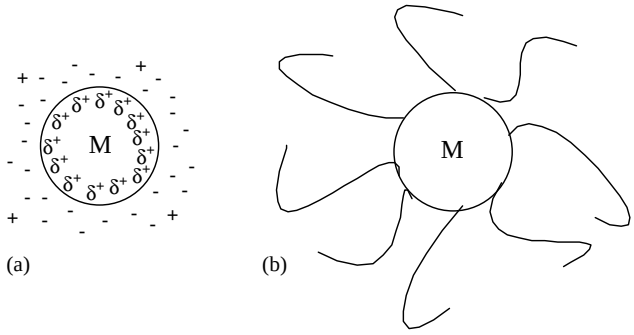

Fig. 1. A schematic illustration for (a) an electrostatically stabilized metal (M) particle (i.e., one stabilized by the adsorption of ions and the resultant electrical multi- ("double") layer), adapted from the literature [7b], and (b) a sterically stabilized metal particle (i.e., one stabilized by the adsorption of polymer chains) [7c].

[1] In the pages to follow, a number of textual footnotes are provided that provide additional insight or detail *for the interested reader*. Most readers may find it easiest to scan or perhaps largely ignore these footnotes in their initial reading, but then refer back to them as necessary or as their interest guides.

[2] The full anion series established elsewhere [1–3] is: $P_2W_{15}Nb_3O_{62}^{9-} \sim [(P_2W_{15}Nb_3O_{61})_2O]^{16-} \sim ([P_2W_{15}(TiOH)_3O_{\sim 59}]^{9-})_n$ ($n = 1, 2$) $\sim SiW_9Nb_3O_{40}^{7-} > HPO_4^{2-} \sim C_6H_5O_7^{3-} > [-CH_2-CH(CO_2^-)-]_n^{n-} \sim OAc^- \sim P_3O_9^{3-} \sim Cl^- \sim OH^-$. It is important to recognize the caveats applying to this series: first, this series applies rigorously only to the Ir(0) nanoclusters in acetone solvent and for Bu_4N^+ counter cations for which it was measured [1–3]. While key aspects of this anions series are expected to hold under broader conditions, this is just now being experimentally tested (Starkey, L., Finke, R.G., unpublished results and experiments in progress). In addition and as discussed elsewhere [1,2], no absolute anion series is expected for all metals and under all reaction conditions [1,2]. The metal, ligand type (e.g., non-oxo ligands) or issues such as hard and soft acid and base considerations, what other ligands are present, what counter cations or polymers are present, the solvent, polymeric additives, or the exact reaction conditions are all expected to have at least some effect on which anionic stabilizer is "best" under the exact conditions employed [3,8]. For example, the solvent is expected by DLVO theory [7] to have a major effect on the stability of nanoclusters, and this is a topic that is a focus of one of our studies in progress.

[3] Note also the concluding statement on p. 87 elsewhere [7b] that "Although electrostatic stability (of colloids) has been one of the oldest and most important issues in colloidal science, the number of studies that are sufficiently systematic and detailed to be useful is limited". We would add that a fundamental flaw in the classical colloidal systems [4] used

repulsion [3a–3c] by added polymers, bulky cations, or, presumably, bulky anions, Fig. 1b (which illustrates the polymer case).[4] Note, however, the complete lack of molecular-level insight provided by the current level of understanding of nanocluster stabilization (Fig. 1).

Possible molecular-level factors which come to mind for the observed anion series include: (a) the basicity (and thus the related σ-donor ligating ability) of each anion as measured by its conjugate acid pK_a; (b) hard/soft considerations [8]; or (c) *geometry factors* that one would expect to be important in the anions coordination to the nanocluster's surface. A key part of the present contribution will be the identification of two geometry factors not previously appreciated in the nanocluster literature, namely (i) a C_3 symmetry, tridentate anion coordination to the metal surface, and (ii) a tridentate ligand-to-metal lattice size-matching component in the anionic stabilizer-to-metal interaction. These insights are significant—they are the first molecular-level insights into how the presently most effective anionic stabilization of metal particles in solution is achieved.

2. A brief overview of three relevant nanocluster papers

It is useful to begin by summarizing briefly three papers[5] from the current nanocluster literature which are particularly relevant to the present contribution [9]. The most relevant paper is Bradley and co-worker's studies, in which they use their CO adsorption plus IR spectroscopy probe. Their work shows that 15 Å, polyvinylpyrrolidone-stabilized Pt nanoparticles do not adsorb CO on the (1 1 1) terrace sites indicated by the light shading in Fig. 2 [10] (Fig. 2 is a reproduction of Fig. 7 provided elsewhere [10]). Those authors postulate that the reason that CO atop (1 1 1) terrace sites is *not* seen is because there are Pt ad-atoms on these sites, as shown by the darker three atoms atop the (1 1 1) terrace in Fig. 2b [10]. Note that such (1 1 1) sites are one place that a tridentate ligand could also sit.

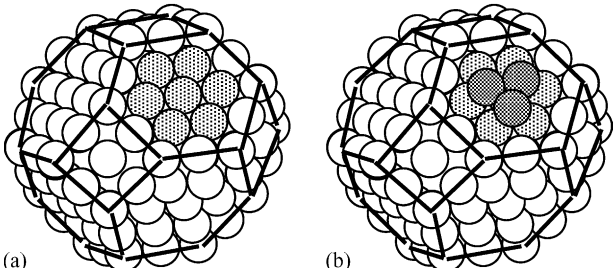

Fig. 2. (a) Regular idealized cuboctahedron with three atoms on an edge and consisting of 201 atoms showing (1 1 1) terraces via shading: note that 56 or 45% of the 122 surface atoms are (1 1 1) terrace sites. (b) The same structure as in (a) but with three ligands or metals added to the (1 1 1) terrace sites (the darker circles). Adapted from Fig. 7 on p. 1271 in Bradley's paper [10].

The second relevant paper, from El-Sayed's laboratories [11a], provides evidence to support the view that capping by polyacrylate^{n-} of the putatively catalytically most active [11b] Pt(1 1 1) faces of tetrahedral (T_d) nanoparticles is what determines the shape of the resultant particles.[6] If capping dominates, then small T_d particles[7] [12] are produced; however, if the Pt(1 1 1) face is not capped (i.e., not poisoned) by polyacrylate^{n-}, then Pt addition to the Pt(1 1 1) face will transform that facet into a Pt(1 0 0) face and, therefore, into intermediate size Pt particles with both (1 0 0) and (1 1 1) faces [11]. Further growth is postulated by the authors to lead, at least in the case of ideal geometry particles, to cubic particles with their six (1 0 0) faces [11]. In short, a picture such as that in Fig. 2 is again implicated.

One general problem, however, with the idealized structural view of nanoclusters employed above is that there is

in such prior work is the lack of precise compositional information for the colloids examined. The use of modern, compositionally well defined nanoclusters for such fundamental studies is imperative, we believe, if one is to exploit the potential present within modern nanoclusters [4].

[4] Suggestive, albeit not definitive, evidence that other factors contribute to the anion series for at least some metal nanoclusters is the classic Pd(0) nanoclusters of Moiseev and co-workers such as $Pd_{\sim 560}L_{\sim 60}(OAc)_{\sim 180}$ (L = 1,10-phenanthroline or 2,2′-bipyridine) or $Pd_{\sim 560}Phen_{\sim 60}O_{\sim 60}(PF_6)_{\sim 60}$ which contain N-based stabilizing ligands as well as O-atom-containing ligands (see the references and discussion on pp. 15–18 elsewhere [4a]). Also noteworthy is that the larger, less symmetric anions in Table 1 with less symmetric charge distributions, such as $P_2W_{15}Nb_3O_{62}{}^{9-}$ polyoxoanion, very likely have effects beyond the unit charge, symmetrical, and therefore considerably more simple anions treated by, and assumed to be point charges in, classical DLVO theory [4a–4c]. Effects which remain to be understood include effects due to whether or not the anion causes more or less electrostriction of the multi-layer surrounding the nanocluster, thereby leading to lower stability, and the effects due to different solvents. In short, there are some basic issues of colloidal-like stabilization and DLVO theory that need to be examined with *poly*anions.

[5] A fourth paper of some interest is one reporting the formation of rods rather than spherical particles in the presence of $NO_3{}^-$ in electrochemically grown Ag(0) nanoclusters [9a]. The molecular basis for this effect was not presented or even considered, however. A fifth paper of some relevance examines the use of citrate^{3-} as a stabilizing agent for Pt particles; these authors find evidence for the same type of Pt(1 1 1) capping effects [11a], this time by citrate, leading to T_d, and then to cubic or truncated O_h, structures as clearly revealed by Figs. 8 and 9 elsewhere [9b]. A sixth paper suggests the binding of both the azabicyclo[222]octane and OH groups in cinchonidine in a Rh nanocluster asymmetric hydrogenation of ethyl pyruvate reduction [9c].

[6] It is not known for certain if the Pt(1 1 1) face is the most active site in the *nanocluster*, as this is an assumption taken from Pt single-crystal work extrapolated to the nanoclusters, as the authors have noted [11b]. Especially in disordered surface-structure nanoclusters, edge, vertex and other sites of higher coordinative unsaturation are likely even more active sites, depending upon the specific reaction catalyzed.

[7] The smaller, T_d nanoparticles seen by TEM for polyoxoanion-stabilized Rh(0) nanoclusters [12] are consistent with the explanation provided by El-Sayed and co-workers for the formation of such T_d particles [11a], binding of $P_2W_{15}Nb_3O_{62}{}^{9-}$ or $[(P_2W_{15}Nb_3O_{61})_2O]^{16-}$ (which the present review reveals should be κ^3–O, i.e., tridentate, $(O)_3$) to an Rh(1 1 1) face of T_d nanoclusters, thereby arresting the growth of (and capturing) these T_d particles.

Table 1
Key data for the five polyanionic, tridentate-oxygen size and size presenting nanocluster-stabilizing anions examined with Ir(0) nanoclusters[a]

Stabilizing anion[b]	k_2/k_1 ratio[c] $\times 10^{-5}$	Nanaocluster dispersity	Are the nanoclusters fully re-dissolvable in acetone?	Catalytic activity after re-dispersion (mmol H_2/h)[e]	TTOs of cyclohexene hydrogenation[f]	**Anions' relative ranking**	Anions' conjugate acid pK_a	O−O distance (Å)[j]	Size-matching[k] (O−O/Ir−Ir)
$P_2W_{15}Nb_3O_{62}^{9-}$	4.4(5)	21(4) Å	Yes	2.2(2)	68000	**First group**	∼9.2	2.85	1.05 (1.09)
$SiW_9Nb_3O_{40}^{7-}$	1.2(1)	22(4) Å	Yes (as a slightly turbid solution)[d]	2.6(3)	41000	**First group**	[Estimate ≤9.2]	2.67	0.98 (1.03)
HPO_4^{2-}	0.072(1)	18(4) Å	Yes	0.8(1)	[≤150000][g]	**Second group**	12.4	2.50	0.92 (0.96)
$Citrate^{3-}$	1.3(1)	18(4) Å	Yes	0.4(1)	[7600][h]	**Second group**	5.4	2.8–3.1	1.03 (1.07) to 1.14 (1.19)
$[P_3O_9]^{3-}$	1.2(1)	(Bulk metal formation)	No	–	[≤82000][g]	**Third group**	N.A.[i]	3.30	1.21 (1.27)
OH^-	0.16(3)	(Bulk metal formation)	No	–	–	**Third group**	15.7	–	–

[a] Data for the columns 2–6 are taken from [1–3] (in the case of HPO_4^{2-}).

[b] Anion entries for the first four anions (i.e., all but $P_3O_9^{3-}$ and OH^-) include 1 eq. of added Proton Sponge™ to consume the 1 eq. of H^+ generated in the reaction; if needed see elsewhere for further details and discussion [1–3].

[c] Kinetic constants from A → B nucleation (rate constant k_1), and A + B → 2B autocatalytic surface growth (rate constant k_2) curve-fits to the sigmoidal H_2 uptake data [1,2].

[d] These $SiW_9Nb_3O_{40}^{7-}$-stabilized nanoclusters are re-dispersable as a nearly clear solution in CH_3CN, results which mean that the slight turbidity observed in acetone is not due to the formation of insoluble bulk Ir(0) metal. Rather, the slight turbidity is most likely due to the inherently lower solubility in acetone of the $SiW_9Nb_3O_{40}^{7-}$ anion as its mixed Na^+/Bu_4N^+ salt (or possibly the presence of a small amount of the tri-Nb–O–Nb bridged $[Si_2W_{18}Nb_6O_{66}]^{8-}$; see the references available elsewhere [1,2]).

[e] Catalytic activity is measured as the rate of hydrogenation, under the standard conditions detailed elsewhere [1,2], of the isolated Ir(0) nanoclusters re-dispersed in acetone.

[f] TTOs are determined for cyclohexene hydrogenation starting with 3.6×10^{-6} mol precursor complex in acetone at 22 °C, 40 ± 1 psig H_2.

[g] These brackets indicate that bulk metal is seen; hence, these TTOs are upper limits to the TTOs of interest for the soluble nanoclusters alone.

[h] This value of 7600 TTOs is probably a lower limit [1,2].

[i] N.A.: not available.

[j] The O−O distances of the three facially coordinating oxygen atoms of the tridentate ligands were calculated from the X-ray structural data: for the heteropolyoxoanion [27] $[P_2W_{15}Nb_3O_{62}]^{9-}$ (three Nb−O−Nb bridging oxygen atoms); for $[SiW_9Nb_3O_{40}]^{7-}$ [29b] (an average of two Nb−O−W and one W−O−W bridging oxygen atom distances); for dihydrogen phosphate [28] $H_2PO_4^-$; for citrate $C_7H_5O_7^{3-}$ (estimated as 3.1 Å from the X-ray structural data [14] of $(NH_4)_5Fe(C_7H_4O_7)_2{\cdot}2H_2O$ by replacing the Fe(III) with Ir(I) at a constant O−M−O angle of ∼90° and using an average Ir−O bond distance of 2.18 Å taken from [30] $(Bu_4N)_2[(1,3\text{-COD})Ir{\cdot}P_3O_9$. Note that the citrate^{3-} ligand is flexible with an O–O bond distance that can probably vary from ca. 2.8–3.1 Å as listed in this table and in Fig. 3. Finally, the O–O distance for trimetaphosphate $[P_3O_9]^{3-}$ was taken from the X-ray structure of $(Bu_4N)_2[(1,3\text{-COD})Ir{\cdot}P_3O_9]$ [30].

[k] Lattice size-matching is defined as how close to 1.0 is the ratio of O−O distance of the tridentate ligand to an Ir−Ir distance of 2.72 Å (or to the 4% contracted value of 2.61 Å, given in parenthesis).

increasing evidence that nanoparticles prepared under a high degree of kinetic control, such as those in Table 1, probably have at least partially amorphous, more disordered structures (i.e., than the idealized structures shown in Fig. 2) at least *initially*, prior to their annealing in the TEM beam which can change their structure to more crystalline forms [4a,11]. Bradley's work [15] is a good place to start for the evidence supporting this claim, for example, see his recent comments regarding the amorphous nature of nanoclusters prepared under kinetically controlled syntheses [10]. Ligand-induced mobility of surface metal atoms may, however, lower the kinetic barrier to forming annealed, smoother surface structures. The exact surface structures and dynamics of transition-metal nanoclusters is an important topic for future research.

The third paper is an interesting contribution from Bradley, Reetz and co-workers in which α-hydroxy carboxylates, such as glycolate, $HOCH_2CO_2^-$, are shown to have an effect on the shape of Pd and Ni nanoclusters [13]. Their results show that the α-hydroxy is required for the effect, but that only a *bidentate* coordination is involved via the α-OH group plus one RCO_2^- carboxylate oxygen (as expected from a consideration of the sp^2 hybridization at the carboxylate carbon and its geometric relationship to the α-hydroxy group: only one lone pair of one carboxylate oxygen atom plus the α-HO group can coordinate simultaneously). The α-HO-RCO_2^- ligand is, then, a net *bidentate*, neutral OH plus O^- donor ligand.

Note that citrate is a different case; the one small molecule structure we could find (a rare structure of a monometallic citrate complex, $[Fe^{III}(citrate^{4-})_2]^{5-}$), shows one α-OH plus two separate RCO_2^- carboxylates donating an oxygen atom each in a net tridentate coordination to Fe(III) [14]. That is, a net *tetra*anionic donor ligand, $citrate^{4-}$, coordinates to the metal via tridentate oxygen donation from one *deprotonated* α-OH plus two RCO_2^- carboxylate oxygens—the latter from *two separate* carboxylates. By inference, tridentate coordination to appropriate geometry nanocluster surfaces is what one expects from citrate. However, when a metal(0) nanocluster is involved (i.e., versus an Fe(III) ion [14b]), the α-OH of citrate is unlikely to be deprotonated[8] until the pH gets above ca. 13–15 [14c]; hence, $citrate^{3-}$ is expected to donate a neutral OH plus two O^- atoms from two separate carboxylates when coordinated to a metal(0) nanocluster surface.

In summary, the key points from an examination of the relevant prior literature are: (a) two papers provide the only prior evidence for higher than unidentate coordination of stabilizing anions to a nanocluster's surface; (b) Bradley's precedent in Fig. 2 is the only prior work which provides one type of site where tridentate anions, such as those emphasized herein, can bind, at least to nanoclusters whose *thermally annealed structures* approach idealized structures such as the fcc cuboctahedron shown in Fig. 2; and (c) the above points are little discussed in the nanocluster literature—that is, there is virtually no molecular detail or surface coordination chemistry in the nanocluster literature save the use of CO as a surface spectroscopic probe in especially Bradley's laboratories [10,15].

3. A concise overview of the key results from interfacial electrochemistry and surface science studies of SO_4^{2-} and HPO_4^{2-} adsorption to M(1 1 1) surfaces (M = Ir, Rh, Pt, Au, Cu)

The specific adsorption of especially $H_pSO_4^{p-2}$ on Pt(1 1 1) and other M(1 1 1) surfaces is a topic of both historical as well as current interest in interfacial electrochemistry and associated surface science literature [16–23].[9] Sulfate adsorption on Pt(1 1 1) and related metals has been studied by a wide range of methods (see references [1–20] elsewhere [18]): conventional electrochemical methods, radiotracer methods [16], electrochemical quartz crystal microbalance methods, spectroelectrochemical methods, scanning tunneling microscopy (STM) [18,22], surface X-ray scattering (SXS), subtractively normalized interfacial Fourier transform infrared spectroscopy (SNI-FT-IRS) [17], computational methods on 50–100-atom clusters (at the HF-MCP level of theory) [23], and by ex situ techniques (i.e., ultra-high vacuum methods) including recent LEED studies [21]. The understanding of the anomalous adsorption peaks and characteristic "butter-fly" cyclic voltammograms [16] when sulfate is present has advanced from Clavilier's first report [24] of these peaks and the (incorrect) early interpretation of the voltammograms as strongly bound H adsorption/desorption peaks [25], through controversies [17–19,24,25] about the actual species being adsorbed, $H_pSO_4^{p-2}$ ($p = 0$ or 1) plus $H_qO^{0/+}$ ($q = 2$ or 3), and through controversies about the interpretation of STM images [19]. The current, relatively high level of understanding of sulfate adsorbed onto transition-metal surfaces is as depicted in Fig. 3, a figure adapted from Itaya and co-workers [22] for the case of SO_4^{2-} plus H_2O co-adsorption onto flame annealed, atomically flat, oxide free Ir(1 1 1), a precedent directly relevant to the Ir(0) nanocluster stabilization studies which will be our focus in a moment.

[8] The α-OH could in principle be deprotonated at pH values that are perhaps 1–3 pK_a units basic than the ROH pK_a due to the pK_a shift expected upon coordination to the electrophilic metal(0) nanocluster surface.

[9] (a) The introduction to reference [17] contains a good discussion, plus references, of the history of the $H_pSO_4^{p-2}$ adsorption on Pt(1 1 1) problem. (b) Reference [18] provides a STM study of the adsorption of sulfate and phosphate on Au(1 1 1) and Au(1 0 0), plus an excellent listing of the methods used in the literature to study the specific adsorption of anions to electrochemical surfaces (see references [1–20] therein [18]). (c) Reference [19] provides an IR study of sulfate/water co-adsorption onto Au(1 1 1). Noteworthy are the citation, and references, therein to the statement that the "interpretations of the observed STM images are controversial" [19].

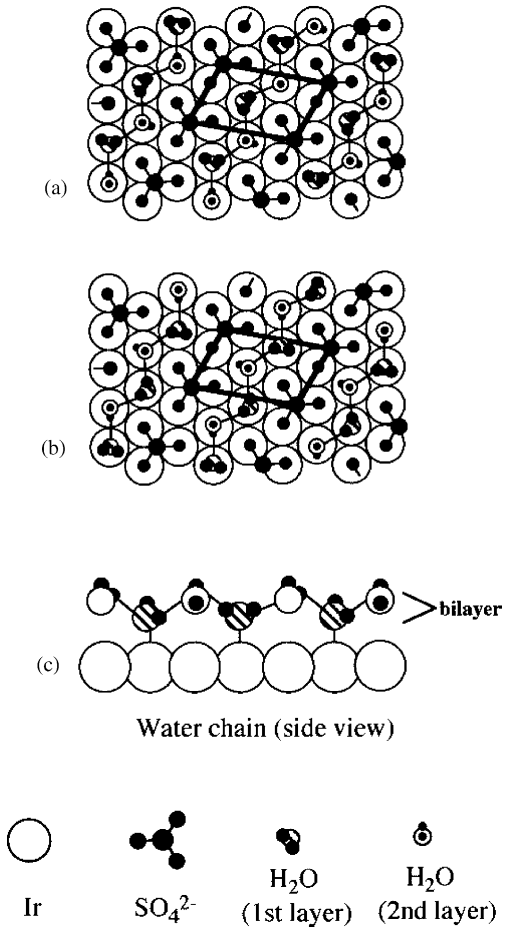

Fig. 3. Schematic illustration of the ($\sqrt{3} \times \sqrt{7}$) adlayer structure of sulfate adsorbed to Ir(1 1 1). (Adapted from Itaya and co-workers' paper [22] with permission.) Water is also co-adsorbed; two possible arrangements of the water H-bonded chains are shown in (a) and (b). The stoichiometry of the fragment of the larger surface shown in (b) is: $1Ir{:}0.2SO_4^{2-}{:}0.37H_2O$. The key feature for the present work is that a tridentate binding of three sulfate oxygens is seen with the C_3 axis of sulfate perpendicular to the plane of the Ir(1 1 1) surface.

The essence of the structural model in Fig. 3 is a so-called ($\sqrt{3} \times \sqrt{7}$) symmetry structure for the adlayer of SO_4^{2-} atop Ir(1 1 1) along with co-adsorption of H_2O in H-bonded chains in-between the rows of sulfate [22]. The distance between adjacent sulfates (the edges of the unit cell in Fig. 3) are $\sqrt{3}a_{Ir}$ (or 4.7 Å) and $\sqrt{7}a_{Ir}$ (or 7.1 Å) in the *A* and *B* directions, respectively (a_{Ir} is the Ir–Ir distance) [22]. The high resolution STM experimentally observed Ir–Ir distance is ~2.7 Å [22], a number that will become important later when we need a good estimate of the Ir–Ir distance atop a $Ir(0)_n$ nanocluster's surface. Note that the sulfate is adsorbed at a three-fold hollow site via three oxygens and with the C_3 axis in the bound SO_4^{2-} perpendicular to the plane of the surface. Note also that this ($\sqrt{3} \times \sqrt{7}$) symmetry structure is "identical with that found previously on Au(1 1 1), Pt(1 1 1), Rh(1 1 1), and Cu(1 1 1)" [22]. Of further interest here is that *phosphate* has been found to bind in a similar structure to Au(1 1 1) [18], sulfate and phosphate, of course, presenting identical tridentate oxo-ligation symmetries. Interestingly, in the Au(1 1 1) case, it was noted that the O–O distance in sulfate (2.47 Å) "is of the same order as the distance between the gold atoms (2.88 Å) and their geometrical arrangement matches that of the Au(1 1 1) surface" [18]. We will refine significantly this early hint at a lattice size-matching requirement intrinsic to the model in Fig. 3 and discovered independently herein[10] by providing the first experimental evidence that matching the tridentate anion metal lattice *much closer* than the above 2.88–2.47 = 0.41 Å difference yields a better nanocluster stabilizer. Finally, a model suggesting a *four-fold symmetry* coordination of even very non-basic anions such as $SiW_{12}O_{40}^{4-}$ in a monolayer onto a Ag(1 1 1) surface [26] has appeared,[11] one that perhaps merits reexamination in light of the preference for three-fold symmetry in the literature cited above.

4. Recent results from Ir(0) nanocluster formation and stabilization studies en route to the ligand-to-metal, tridentate anion-binding lattice size-matching model/hypothesis

Fig. 4 shows X-ray diffraction established structures [27–30] of the coordination sites of each of the more effective anionic stabilizers from the anion series [1–3] $P_2W_{15}Nb_3O_{62}^{9-} \sim SiW_9Nb_3O_{40}^{7-} > HPO_4^{2-} \sim C_6H_5O_7^{3-} > P_3O_9^{3-}$. The X-ray diffraction determined structure of $(C_5Me_5)Rh{\cdot}P_2W_{15}Nb_3O_{62}^{7-}$ [27a] and ^{17}O and ^{183}W NMR-determined structure of $(1,5\text{-COD})Ir{\cdot}P_2W_{15}Nb_3O_{62}^{8-}$ [27b,27c] both show the κ^3–O (i.e., tridentate O-donating) nature of the $P_2W_{15}Nb_3O_{62}^{9-}$ polyoxoanion, for example. Note that the above anion series includes HPO_4^{2-}, an anion which *was predicted*, as part of the present work and on the basis of Fig. 4, to be an effective stabilizer and then tested experimentally elsewhere [3] by the five criteria [1] leading to the data for HPO_4^{2-} summarized in row 3 of Table 1.

The first, fundamental insight from Fig. 4 and the data in Table 1, then, is that each of these to-date premier anionic stabilizers of transition-metal nanoclusters presents a tridentate, facial array of oxygen atoms for coordination to a transition-metal(0) nanocluster's surface. The results in Table 1, plus the structurally established single-metal

[10] The tridentate oxoanion coordination model for nanoclusters presented herein was discovered before we discovered the interfacial electrochemistry literature of SO_4^{2-} and other anions binding to Pt(1 1 1). Although intellectually somewhat less efficient, this has proven useful in that it provides confidence in the model presented herein and provides independent support for the binding model in the interfacial electrochemistry literature.

[11] Note that the non-basic $SiW_{12}O_{40}^{4-}$ is structurally really $[(SiO_4^{4-})\text{-}(W_{12}O_{36})^0]^{4-}$ and thus formally contains near zero anionic-charge density at its surface, yet still binds to the Ag(1 1 1) surface [26a,26b]. An interesting question is whether or not *tridentate* binding of $SiW_{12}O_{40}^{4-}$ to Ag(1 1 1) might not be possible at coverages below a monolayer.

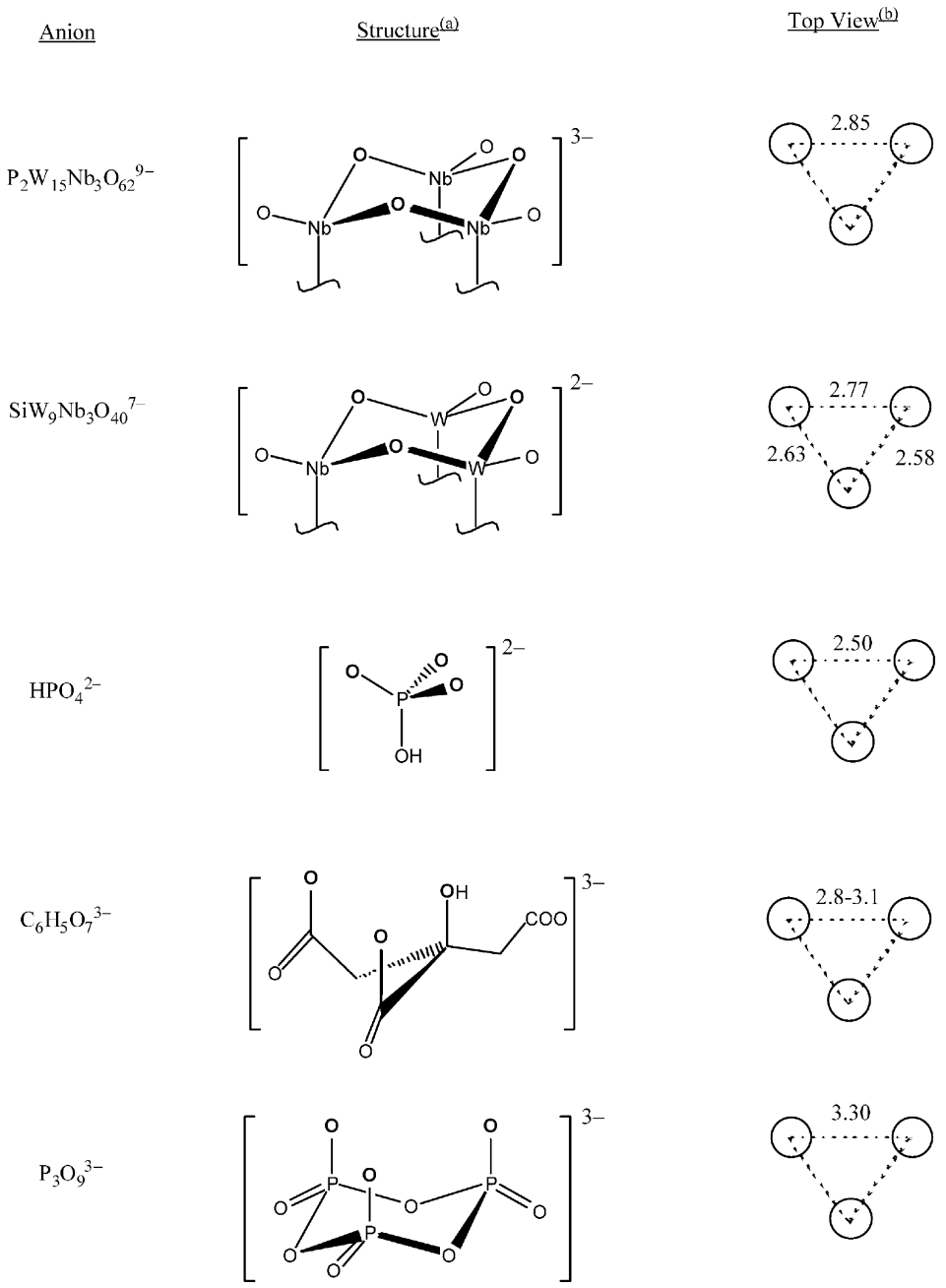

Fig. 4. Structure and top view of six polyanions: (a) only the structure of coordinating part of the top two polyoxoanions is shown; (b) top view as seen by the iridium surface. The O−O distances (in Å) of the three facially coordinating oxygen atoms of the tridentate ligands were calculated from the X-ray structural data for the polyoxoanion [27] $[P_2W_{15}Nb_3O_{62}]^{9-}$ (three Nb−O−Nb bridging oxygen atoms), for the polyoxoanion [29b] $[SiW_9Nb_3O_{40}]^{7-}$ (note the small differences between the two Nb−O−W and one W−O−W bridging oxygen atom distances), hydrogenphosphate [28] HPO_4^{2-} (estimated from the structure of dihydrogenphosphate, $H_2PO_4^-$); citrate $C_7H_5O_7^{3-}$ (estimated from the X-ray structural data [14] for $(NH_4)_5Fe(C_7H_4O_7)_2{\cdot}2H_2O$) by replacing the Fe(III) with Ir(I) at the constant O−M−O angle = ∼90°, and using the average Ir−O bond distance of 2.18 Å as in the iridium(I) complex [30] $(Bu_4N)_2[(1,3\text{-COD})Ir{\cdot}P_3O_9]$. Note that O−O distances in the iron(III) citrate complex are unequal (2.85, 2.80, and 2.76 Å); note also that one expects that the O−O distance for citrate binding can vary from metal to metal because of flexible structure of the citrate ligand. Lastly, the O–O distance for trimetaphosphate $[P_3O_9]^{3-}$ was taken from the X-ray structure of $(Bu_4N)_2[(1,5\text{-COD})Ir{\cdot}P_3O_9]$ [30].

tridentate coordination modes shown in Fig. 4—as well as the interfacial electrochemistry and surface science literature cited above—strongly suggest that a tridentate coordination is not only preferred, but also leads to the highest nanocluster stabilizing abilities presently known. This is an important, previously unappreciated insight. The important task remains, however, of obtaining *direct* evidence for the proposed tridentate mode of coordination of these anions to clean [4] transition-metal nanocluster surfaces.

The second new, fundamental molecular insight for the nanocluster area comes from examining the data in Table 1 for each of the anions in Fig. 4. Table 1 includes the data according to the five criteria (columns 2–6) for each anion, the data for simple OH^- for comparison, as well as each anion's conjugate acid pK_a in column 8, and each anion's relative ranking for its nanocluster formation and stabilization ability, column 7.

One easily drawn conclusion from the data in Table 1, columns 7 and 8, is that while basicity is important as expected (i.e., increased basicity, and thus increased σ-donation, should lead to higher Ir-O bond energies), basicity is not everything: the most basic but monodentate anion, OH^-, is at the *bottom* of the Ir(0) nanocluster stabilizing anions list. In addition, the two anions with the top ranking ($P_2W_{15}Nb_3O_{62}^{9-}$ and $SiW_9Nb_3O_{40}^{7-}$) are at least 3 pK_a units less basic than one of those (HPO_4^{2-}) in the second rank, and the two anions in the second rank ($HPO_4^{2-} \sim C_6H_5O_7^{3-}$) differ by 7 p$K_a$ units yet are in the same rank—in short, some additional factor is important in setting the relative anion efficacy for the formation and stabilization of the transition-metal nanoclusters.

Further perusal of the data in Table 1 reveals a third, previously unappreciated and important insight even when considering the interfacial electrochemistry and surface science literature cited earlier: the match between the O–O distance in the coordinating anion versus the surface Ir(0)—Ir(0) distance[12] [31] correlates rather well with the anion's relative ranking as a stabilizer. Specifically, anions with a 0.98–1.05 (O–O)/(Ir–Ir) size-matching ratio rank first (column 7, Table 1), while those with a broader, 0.92–1.14 (O–O)/(Ir–Ir) size-matching ratio rank second (and if one uses the larger, 3.1 Å, O–O distance for the flexible citrate). In addition, the anion with the worst match ($P_3O_9^{3-}$; a 1.21 (O–O)/(Ir–Ir) size-matching ratio) is the worst stabilizer. In short, this correlation is prima facie evidence for a geometric, anion-to-surface-metal, lattice-size-matching component to the anion stabilization series summarized in Table 1. All other factors being equal, the preferred tridentate oxoanion nanoclusters stabilizers in Table 1 are those that have the better match between the ligand O–O and surface Ir–Ir distances.

5. Testable predictions of the ligand-to-metal lattice size-matching model/hypothesis

The lattice size-matching model/hypothesis has several testable predictions. The first prediction is:

(i) That HPO_4^{2-} will be a good, previously unappreciated stabilizer for transition-metal nanoclusters with a metal-metal distance of ca. 2.50 Å that, therefore, matches reasonably well with the HPO_4^{2-} O–O distance. This prediction has already been tested [3] and found to be true (the data in Table 1, row 3; see elsewhere for the full details of that work [3]). The experimental confirmation of this prediction provides strong support for the lattice size-matching model/hypothesis.

Several additional testable predictions of the lattice size-matching model are listed below. While experiments to test several of the predictions below are underway in our labs, we welcome the efforts of others to perform their own experiments testing this new, working model/hypothesis.

(ii) The next prediction is, of course, that direct structural methods will find evidence for tridentate coordination to transition-metal nanocluster surfaces. The place to start here would seem to be clean single crystal surfaces to which the anions from the above series are individually added and investigated with physical methods such the various microscopies and LEEDS if possible. Different metals, with the different anions, are all of interest. We hope others, who have the specialized equipment and capabilities required, will undertake the needed, interesting experiments. IR studies of $Ir(0)_n \cdot (HPO_4^{2-})_b$ nanoclusters, analogous to those done with SO_4^{2-} on single crystal surfaces, should exhibit a characteristic IR band [17,19] and, hence, are also of interest. Such studies will, however, first require the synthesis and characterization of $Ir(0)_n \cdot (HPO_4^{2-})_b$ nanoclusters [3] (i.e., where "*b*" in the above formula is a minimum so that only surface-bound HPO_4^{2-} is present).

(iii) The third testable prediction is that CO and Bradley's CO/IR methodology [10,15] can be used to see whether or not tridentate anions sit at sites such as those indicated in Fig. 2b. The prediction is that bands for CO will not be seen for surface sites where tridentate anions are already sitting. Controls will need to be done

[12] (a) The Ir–Ir distance is estimated as 2.72–2.61 Å (the latter value if one subtracts the precedented ca. 4% surface contraction, vide infra); a measurement of the Ir–Ir distance on single crystal Ir yields an experimental value of ∼2.7 Å [22]. However, the metal-metal distance on the surface of Ir nanoclusters is not known exactly. It is expected to be a few percent less than the distance in bulk Ir of Ir–Ir = 2 × 1.36 Å = 2.72 Å for the following reasons: several EXAFS studies show that the surface metal-metal distance is contracted ca. 1–4% versus the bulk value in most metal particles, for example the surface metal–metal distances are contracted only 1.0–1.5% for three supported Ru particle samples examined by EXAFS [31a], 4 ± 1% in an $Au_{\sim 55}(PPh_3)_{\sim 12}Cl_{\sim 6}$ cluster examined by EXAFS [31b], and 3.8% in $Pd_{\sim 400}phen_{\sim 400}OAc_{\sim 800}H_{\sim 1600}$ also based on EXAFS data [31c]. This contraction is just what one expects for the lower coordination number (and enhanced metal-metal multiple bonding) at the surface, plus perhaps a contribution to contraction from the anion-stabilizer-induced partial positive, surface charge-mirror [31e]. Of interest is that this contraction is smaller than the 15% contraction seen for the *naked* Ir(1 1 0) single crystal surface [31d,31f,31g] (1.16 Å versus the 1.36 Å Ir radius in bulk Ir); the 1.0–1.5% contraction noted above is also smaller than the 5% contraction on a Ni(1 1 0) single crystal surface [31d]. Measurement of the additional surface M–M distances, as a function of the nanocluster size, ligands, and other variables, as well as for individual surface facets if possible, would seem to be an important objective for future EXAFS research.

without those anions, and with monodentate anions, to bolster confidence that the results have been correctly interpreted.[13]

(iv) A fourth, testable prediction concerns which tridentate anions will be the best stabilizers for different transition-metals. Considering the common nanocluster metals of Groups 9–11 and which crystallize in a ccp structure as does Ir(0), their metallic diameters (2 × their radii in Å) are: Co (2 × 1.25 = 2.50), Rh (2 × 1.34 = 2.68), Ir (2 × 1.36 = 2.72), Ni (2 × 1.25 = 2.50), Pd (2 × 1.37 = 2.74), Pt (2 × 1.39 = 2.78), Cu (2 × 1.28 = 2.56), Ag (2 × 1.44 = 2.88), and Au (2 × 1.44 = 2.88). The $P_2W_{15}Nb_3O_{62}^{9-}$ polyoxoanion with its 2.85 Å O−O distance has been shown to be the best stabilizing anion for Ir(0) nanoclusters [1] and also an excellent stabilizer for Rh(0) nanoclusters [32]. The smaller HPO_4^{2-} anion (2.52 Å O−O distance) is expected to be a better stabilizer for nanoclusters of the smaller metals such as Co, Ni, and Cu, all other factors, such as anion basicity, being equal. The best stabilizer for nanoclusters of the larger metals such as Ag and Au are predicted to require tridentate anions with a longer O−O distance, for example, the $P_2W_{15}Nb_3O_{62}^{9-}$ polyoxoanion with its O–O distance of 2.85 Å or the $citrate^{3-}$ anion with its flexible 2.8–3.1 Å O–O distance. It is noteworthy here that citrate is, of course, one of the oldest and most often utilized stabilizers of Au nanoclusters [33], the reasons why were not previously apparent, however. The $P_2W_{15}Nb_3O_{62}^{9-}$ polyoxoanion is predicted to be a top stabilizing agent for Pt(0) nanoclusters since the Pt−Pt (2.78 Å) distance is only slightly larger than the Ir−Ir distance (2.72 Å). Other such predictions for other anions and metals are of course possible. Significantly, each of these predictions for the different metals are testable by the general methods and five criteria [1,2] utilized herein. Of note here is that the finding of the $(\sqrt{3}\times\sqrt{7})$ symmetry structure for tridentate anions on Rh(1 1 1), Pt(1 1 1), and Au(1 1 1) as well as Ir(1 1 1) [16–23] provides high confidence in the prediction that nanoclusters of these particular metals will be well stabilized by tridentate anions correctly picked to include a good size-matching component.

(v) Other testable predictions of the C_3 symmetry, lattice size-matching model that we have not thought of are undoubtedly possible as well. Again, we hope others will join our efforts to support, refute or refine this working model.

One very important corollary of the C_3 symmetry, lattice size-matching model, then, is the ability to chose, up-front and thus *by design*, a subgroup of 2–3 of the best anionic stabilizers to try initially in the synthesis of a given transition-metal nanocluster. This is a *significant advance* in the nanocluster area where, until very recently [1,2], the anion was often *neglected* since the cation was claimed, incorrectly, to be more important than the anion in nanocluster stabilization (see the discussion of this point available elsewhere [1,2]). In addition, previously there was no idea of which anions were the best choices—in fact, the choice of anionic stabilizer was typically not a question that was even considered. Most of the anions commonly used to date (Cl^-, OAc^-, $polyacrylate^{n-}$; or even $citrate^{3-}$) are not the best stabilizers compared to the present, top stabilizing anions such as $P_2W_{15}Nb_3O_{62}^{9-}$ [1]. The addition of the reductively relatively stable, ^{31}P NMR handle containing, cheap and readily available HPO_4^{2-} to the arsenal of preferred anions for stabilizing transition-metal nanoclusters is an important result in its own right [3].

6. Caveats

Finally, the caveats already mentioned merit re-emphasis, namely those related to the anion series[2] on which the present work is based, plus the caveat that only thermally annealed nanoclusters are likely to approach the idealized structures shown in Fig. 2 [14]. Overall, however, the results in this paper begin to provide some of the previously missing foundation from which to launch more rational studies focused at developing even better anionic stabilizers for transition-metal nanoclusters. This includes tridentate stabilizers employing elements other than oxygen, as well as the rational design of stabilizers that might more effectively promote asymmetric synthesis reactions of transition-metal nanoclusters.

7. Summary

In summary, the ten most important findings from the present work are:

(i) The presently premier anionic stabilizers of transition-metal(0) nanoclusters present a tridentate, facial array of oxygen atoms for coordination to the metal(0) surface.

(ii) The preferred tridentate oxoanion stabilizers of nanoclusters are those that have the best match between the ligand O–O and surface Ir–Ir distances, all other factors being equal—that is, there is a pre-

[13] Such controls are needed since these IR experiments can yield negative results in the cases where, for example, no band for the terrace sites in Fig. 2b can be observed. However, in the ideal case with a low concentration of anionic stabilizer to start, the bands for all the sites should be observable so that the bands characteristic of where the stabilizer sits can be titrated away as more and more anionic stabilizer is added and the Ir–CO IR band is monitored. To start, it would seem prudent that these studies use the clean-surface nanoclusters that are now available [4] and that one work with the most ordered, higher-temperature-annealed, structures that one can make. Then, the more challenging problem of disordered nanocluster structures in solution could be examined. Such structural studies using the methods that are now available [15] are badly needed; hence, they are a part of our in-progress studies.

viously unappreciated, geometric, anion-to-surface-metal, lattice-size-matching component to the best anionic stabilizers of transition-metal nanoclusters, an effect precedented in the literature of SO_4^{2-} binding to M(1 1 1) surfaces (M = Ir, Rh, Pt, Au, Cu). These are important molecular-level insights for how the to-date premier tridentate, anionic stabilizers of transition-metal nanoclusters achieve their higher level of stabilization—a non-trivial advance since there was previously a complete lack of molecular-level insights into how transition-metal nanoclusters are stabilized.

(iii) HPO_4^{2-} was predicted, then experimentally verified, to be a heretofore unappreciated, simple, effective and readily available stabilizer of Ir(0) and other transition-metal nanoclusters where there is a lattice-size match between the HPO_4^{2-} O–O and surface M–M distances. This rationally discovered new nanocluster stabilizer was shown to be as good a stabilizer as the commonly employed citrate^{3-}.

The C_3 symmetry, lattice size-matching model is significant in seven additional ways:

(iv) The five tridentate oxoanions in Fig. 4 provide a new tool for the study of oxoanions bound to metal surfaces. For example, $P_2W_{15}Nb_3O_{62}^{9-}$ is predicted to be an additional, tighter binding ligand than the better studied SO_4^{2-} for use in interfacial electrochemistry studies; further investigations of the tighter binding, but also lesser studied [18], HPO_4^{2-} are suggested as well. Note here how quickly, using the structurally precise ligands in Fig. 4, we were able to discover and report in a single paper the current C_3 symmetry, tridentate oxoanion coordination, lattice size-matching model (cf. to the multitude of papers, using many sophisticated physical methods, from the interfacial electrochemistry and associated surface science literature, including the controversies in that literature cited earlier [17–19,24,25]).

(v) The results herein are for compositionally well-defined ligands and nanoclusters, and as such do not suffer from the ambiguities, and resultant controversies, of the surface bound SO_4^{2-} literature, namely the uncertainties about the protonation state of the exact adsorbing species, $H_pSO_4^{p-2}$ ($p = 0$ or 1) plus $H_qO^{0/+}$ ($q = 2$ or 3).

(vi) The results support suggestions in the literature by El-Sayed and coworkers that capping, and thereby poisoning growth on, M(1 1 1) surfaces should achieve shape-controlled growth of nanoclusters [11].

(vii) The results provide further evidence disproving the persistent myth[14] [1,2] that R_4N^+ *cations* absorb directly to M(0) nanocluster electrophilic surfaces and are more important in nanocluster stabilization than are surface-adsorbed anions. It is time to abandon this myth [34]!

(viii) The deduction of the C_3 symmetry, lattice size-matching model from the anion-efficacy series, and its verification by virtually identical findings from the interfacial electrochemistry surface science literature, show that the methods and five criteria for rating nanocluster stabilizers first detailed elsewhere [1]—the first such methods—*are reliable* and thus a significant advance.

(ix) The finding that the same, so-called ($\sqrt{3} \times \sqrt{7}$) symmetry structure is found for adsorbed tridentate oxoanions (e.g., for SO_4^{2-}) on Rh(1 1 1), Pt(1 1 1), Au(1 1 1), and Cu(1 1 1) ensures that the tridentate oxoanion binding and stabilization preferences discovered herein for Ir will translate to at least these other metal nanoclusters when M(1 1 1) facets are present and if a tridentate oxoanion with a good metal-lattice size match is chosen as a stabilizer.

(x) And finally,[15] the results provide molecular-level insight to guide the ill-understood area of phosphating of metal surfaces [35] to achieve corrosion resistance, electrical resistance, or to achieve bonding to organic coatings such as rubber. The present results provide the first evidence suggesting a tridentate mode of phosphate and similar anion binding to metal surfaces during phosphating for corrosion resistance. Previously, "P–O$^-$" as the monodentate binding unit [35b] was as far as molecular understanding in phosphating of metal surfaces had progressed, despite the importance of the phosphating process, for example the fact that "almost all car and van body components made in the world today are phosphated before painting" [35a]. Another insight is that HPO_4^{2-} should prefer the metals where there is a good lattice size-match, especially Co, Ni, and Cu, but also Fe, Ru, Rh Ir, Pd, Re, Os, and Pt (see footnote 28 elsewhere [3]). In addition, the findings herein foretell the use of each of the ligands in Fig. 4, plus their custom-made derivatives, in the areas of metal surface treatment for enhanced material properties.

Note added in proof

Two interesting papers by Shapley and co-workers describe the crystallographically characterized, organometallic tri-metal cluster complexes, $H_2Os_3(CO)_9(\mu_3,\eta^3\text{-}O_3ER)$ (ER = PR; SO; AsR) [36,37]. The $\mu_3,\eta^3\text{-}O_3ER$ bonding to the triangular Os_3 core which is structurally characterized

[14] A referee cited (the myth that) R_4N^+ cations adsorb tightly to a metal surface, referencing a well known electrochemical text which cites this myth [34]. Examination of the data cited [34] shows that it, too, suffers from neglect of the anions present—which are undoubtedly adsorbed first to the electrode surface (see elsewhere [1] for further discussion of the other issues here).

[15] Actually, there is one more conclusion: if, for a given reaction, a M(1 1 1) facet is in fact kinetically dominant [11b] in a nanocluster, then capping agents which do *not* bind to that M(1 1 1) surface should yield even faster, and perhaps also different selectivity, catalysts.

by Shapley and co-workers is a molecular analog of the C_3 symmetry, lattice size-matching model detailed in the present contribution.

Acknowledgements

We thank Prof. John Bradley for sharing an electronic copy of his original Fig. that was used to make Fig. 2 herein. An anonymous referee is thanked for sharing their expert knowledge of the literature of $H_pSO_4^{p-2}$ on M(1 1 1) surfaces. Support for this research was provided by the Department of Energy, Office of Basic Energy Sciences, via DOE grant FG06-089ER13998.

References

[1] S. Özkar, R.G. Finke, J. Am. Chem Soc. 124 (2001) 5796.
[2] S. Özkar, R.G. Finke, Langmuir 18 (2002) 7653.
[3] S. Özkar, R.G. Finke, Langmuir 19 (2003) 6347.
[4] For two introductory reviews, lead references to earlier reviews and needed definitions (e.g., of modern transition metal nanoclusters vs., for example, classical colloids), see:
(a) J.D. Aiken III, R.G. Finke, J. Mol. Catal. A: Chem. 145 (1999) 1;
(b) J.D. Aiken III, Y. Lin, R.G. Finke, J. Mol. Catal. A: Chem. 114 (1996) 29–51;
(c) R.G. Finke, Transition-metal nanoclusters: solution-phase synthesis, then characterization and mechanism of formation, of polyoxoanion- and tetrabutylammonium-stabilized nanoclusters, in: D.L. Feldheim, C.A. Foss Jr. (Eds.), Metal Nanoparticles: Synthesis, Characterization and Applications, Marcel Dekker, New York, 2002, Chapter 2, pp. 17–54.
[5] Other lead reviews:
(a) G. Schmid, M. Baumle, M. Geerkens, I. Heim, C. Osemann, T. Sawitowski, Chem. Soc. Rev. 28 (1999) 179;
(b) G. Schmid, L.F. Chi, Adv. Mater. 10 (1998) 515;
(c) J.H. Fendler (Ed.), Nanoparticles and Nanostructured Films, Wiley-VCH, Weinheim, 1998;
(d) A. Fürstner (Ed.), Active Metals: Preparation, Characterization, and Applications, VCH, Weinheim, 1996;
(e) J.S. Bradley, in: G. Schmid (Ed.), Clusters and Colloids: From Theory to Applications, VCH, New York, 1994, pp. 459–544;
(f) G. Schmid, Chem. Rev. 92 (1992) 1709.
[6] For an introduction to the mechanisms of transition-metal nanocluster formation, including a comprehensive listing of the prior literature in the area, see:;
(a) M.A. Watzky, R.G. Finke, J. Am. Chem. Soc. 119 (1997) 10382, and references therein;
(b) M.A. Watzky, R.G. Finke, Chem. Mater. 9 (1997) 3083;
(c) J.D. Aiken III, R.G. Finke, J. Am. Chem. Soc. 120 (1998) 9545, and references therein to diffusive agglomeration of nanoparticles;
(d) J.A. Widegren, J.D. Aiken III, S. Özkar, R.G. Finke, Chem. Mater. 13 (2001) 312, and references therein.
[7] (a) D.F. Evans, H. Wennerström, The Colloidal Domain, second ed., Wiley-VCH, New York, 1999;
(b) C.S. Hirtzel, R. Rajogopalan, Colloidal Phenomena: Advanced Topics, Noyes Publications, Park Ridge, NJ, 1985, pp. 27–39, 73–87;
(c) R.J. Hunter, Foundations of Colloid Science, vol. 1, Oxford University Press, New York, 1987, pp. 316–492.
[8] References to hard–soft correlations:;
(a) J.E. Huheey, E.A. Keiter, R.L. Keiter, Inorganic Chemistry, Principle of Structure and Reactivity, fourth ed., Harper-Collins College Publishers, New York, 1993, p. 347, Table 9.7;
(b) R.G. Pearson, Inorg. Chem. 27 (1988) 734, Chem. Br. (1991) 441.
[9] (a) Y.-Y. Yu, S.-S. Chang, C.-L. Lee, C.R.C. Wang, J. Phys. Chem. B 101 (1997) 6661;
(b) A. Henglein, M.J. Giersig, Phys. Chem. B 104 (2000) 6767;
(c) Y. Huang, J. Chen, H. Chen, R. Li, Y. Li, L. Min, X. Li, J. Mol. Catal. A: Chem. 170 (2001) 143.
[10] See the data for the particles denoted Pt-15: D. De Caro, J.S. Bradley, N. J. Chem. (1998) 1267.
[11] (a) J.M. Petroski, Z.L. Wang, T.C. Green, M.A. El-Sayed, J. Phys. Chem. B 102 (1998) 3316;
(b) T.S. Ahmadi, Z.L. Wang, T.C. Green, A. Henglein, M.A. El-Sayed, Science 272 (1996) 1924.
[12] J.D. Aiken III, R.G. Finke, Chem. Mater. 11 (1999) 1035.
[13] J.S. Bradley, B. Tesche, W. Busser, M. Maase, M.T. Reetz, J. Am. Chem. Soc. 122 (2000) 4631.
[14] M. Matzapetakis, C.P. Raptopoulou, A. Tsohos, V. Papaefthymiou, N. Moon, A. Salifoglou, J. Am. Chem. Soc. 120 (1998) 13266.
[15] (a) D. De Caro, J.S. Bradley, Langmuir 14 (1998) 245;
(b) D. De Caro, J.S. Bradley, Langmuir 13 (1997) 3067;
(c) J.S. Bradley, E.W. Hill, B. Chaudret, A. Duteuil, Langmuir 11 (1995) 693;
(d) J.S. Bradley, J.M. Millar, E.W. Hill, C. Klein, B. Chuderet, A. Duteuil, J.W. Gesu, R.W. Joyner, P. Foulloux, P.A. Sermon, M. Ichikawa, F. Bozonverduraz, Stud. Surf. Sci. Catal. 13 (1997) 3067.
[16] A. Kolics, A. Wieckowski, J. Phys. Chem. 105 (2001) 2588, and references cited therein.
[17] P.W. Faguy, N. Markovic, R.R. Adzic, C.A. Fierro, E.B. Yeager, J. Electoanal. Chem. 289 (1990) 245.
[18] A. Cuesta, M. Kleinert, D.M. Kolb, Phys. Chem. Chem. Phys. 2 (2000) 5684.
[19] K. Ataka, M. Osawa, Langmuir 14 (1998) 951.
[20] M. Kleinert, A. Cuesta, L.A. Kibler, D.M. Kolb, Surf. Sci. 430 (1999) L521.
[21] Y. Shingaya, M. Ito, Phys. Electrochim. Acta 44 (1998) 745.
[22] L.-J. Wan, M. Hara, J. Inukai, K. Itaya, J. Phys. Chem. B 103 (1999) 6978.
[23] P.P. Olivera, M. Patrito, H. Sellers, in: A. Wieckowski (Ed.), Interfacial Electrochemistry: Theory, Experiment and Applications, Marcel Dekker, New York, 1999, Chapter 5, pp. 63–81.
[24] J. Clavilier, R. Faure, G. Guinet, R.J. Durand, Electroanal. Chem. 107 (1980) 205.
[25] (a) J. Clavilier, A. Rodes, K.El. Achi, M.A. Zamakhchari, J. Chim. Phys. 88 (1991) 1291;
(b) N. Furuya, S. Kiode, Surf. Sci. 220 (1989) 18.
[26] (a) M. Ge, B. Zhong, W. Klemperer, A.A. Gerwith, J. Am. Chem. Soc. 118 (1996) 5851;
(b) G. Maohui, A.A. Gerwith, W.G. Klemperer, C.G. Wall, Pure Appl. Chem. 69 (1997) 2175.
[27] (a) M. Pohl, Y. Lin, T.J.R. Weakley, K. Nomiya, M. Kaneko, H. Weiner, R.G. Finke, Inorg. Chem. 34 (1995) 767;
(b) M. Pohl, R.G. Finke, Organometallics 12 (1993) 1453;
(c) M. Pohl, D.K. Lyon, N. Mizuno, K. Nomiya, R.G. Finke, Inorg. Chem. 34 (1995) 1413.
[28] The X-ray diffraction determined structure of $H_2PO_4^-$: A. Boukhris, C. Lecomte, B. Wyncke, F. Brehat, A.J. Thalal, Phys. Condens. Matter 6 (1994) 2475
[29] (a) The X-ray diffraction determined structure of $SiW_9Nb_3O_{40}^{7-}$: K. Nomiya, T. Hasegava, R. Noguchi, K. Nomura, M. Takahashi, H.J. Yokoyama, Chem. Lett. (2001) 1278;
(b) The NMR-determined structure (1,5-COD)Ir·$SiW_9Nb_3O_{40}^{5-}$:Y. Lin, K. Nomiya, R.G. Finke, Inorg. Chem. 32 (1993) 6040.
[30] The X-ray diffraction determined structure of $[(1,5\text{-COD})Ir{\cdot}P_3O_9]^{2-}$: V.W. Day, W.G. Klemperer, D.J. Main, Inorg. Chem. 29 (1990) 2345.
[31] (a) H. Kuroda, T. Yokoyama, K. Asakura, Y. Iwasawa, Faraday Discuss. 92 (1991) 189;
(b) M.C. Fairbanks, R.E. Benfield, R.J. Newport, G. Schmid, Solid State Commun. 73 (1990) 431;

(c) M.N. Vargaftik, V.P. Zargorodnikov, I.P. Stolarov, I.I. Moiseev, V.A. Likholobov, D.I. Kochubey, A.L. Chuvilin, V.I. Zaikosvsky, K.I. Zamaraev, G.I. Timofeeva, J. Chem. Soc., Chem. Commun. (1985) 937–939;
(d) W.H. Weinberg, Survey Progr. Chem. 10 (1983) 1;
(e) K. Christmann, G.Z. Ertl, Naturforsch. A 28A (1973) 1144;
(f) K. Johnson, Q. Ge, S. Titmuss, D.A. King, J. Chem. Phys. 112 (2000) 10460;
(g) C.-M. Chan, M.A. Van Hove, W.H. Weinberg, E.D. Williams, Surf. Sci. 91 (1980) 440.

[32] (a) J.D. Aiken III, R.G. Finke, Chem. Mater. 11 (1999) 1035;
(b) J.D. Aiken III, R.G. Finke, J. Chem. Soc. 121 (1999) 8803;
(c) T. Nagata, M. Pohl, H. Weiner, R.G. Finke, Inorg. Chem. 36 (1997) 1366.

[33] Early use of citrate to stabilize colloids:
(a) J.J. Turkevich, Chem. Phys. 13 (1945) 235;
(b) J. Turkevich, P.C. Stevenson, J. Hillier, Discuss. Faraday Soc. 11 (1951) 55;
J. Turkevich, G. Kim, Science 169 (1970) 873;
(c) P.-A. Brugger, P. Cuendet, M. Grätzel, J. Am. Chem. Soc. 103 (1981) 2923;
(d) See also references [3a–c] in: Y. Lin, R.G. Finke, J. Am. Chem. Soc. 116 (1994) 8335.

[34] A.J. Bard, L.R. Fulkner, Electrochemical Methods, Fundamental and Applications, second ed., Wiley, New York, 2001, p. 545.

[35] (a) W. Rausch, The Phosphating of Metal Surfaces, ASM International, Metals Park, OH, Finishing Publications Ltd., Teddington, Middlesex, England, 1990, ISNB-0-904477-11-8;
(b) T. Lu, L. Li, C.T. Lin, J. Phys. Chem. 99 (1995) 7613;
(c) L.A. Kozlov, V.V. Okulov, "AVTOBAZ", Tolyatti, Russia. Gal′vanotekhnika i Obrabotka Poverkhnosti 7 (2) (1999) 27–32 (Phosphating Theory and Practice, in Russian, CAN 132:254222);
(d) T.R. Giles, Metal Finishing 99 (9) (2001) 10–12, 14–16, 18–20 (Pretreatment of Various Substrates Prior to Electrocoating, Henkel Surface Technologies, Henkel Corp., Madison Heights, MI, CAN 135:306595);
(e) H. Schuemichen, Interfinish 92: International Congress on Surface Finishing, vol. 2, 1992, pp. 630–639 (New Developments in the Field of Phosphating Metal Surfaces, Assoc. Bras. Trat. Superficie, Sao Paulo, Brazil, CAN 119:165228).

[36] R.L. Keiter, D.S. Strickland, S.R. Wilson, J.R. Shapley, J. Am. Chem. Soc. 108 (1986) 3846.

[37] G.R. Frauenhoff, J.-C. Liu, S.R. Wilson, J.R. Shapley, J. Organomet. Chem. 437 (1992) 347.